Large dynamic range optical cavity based sensor using a low cost three-laser system*

Donggee Rho and Seunghyun Kim, *Member, IEEE*

***Abstract*— An optical cavity based biosensor using a differential detection method has been proposed to provide a novel approach to point-of-care diagnostics. A two-laser based optical cavity based sensor system is designed and experimentally demonstrated. While the calculated differential value of the two-laser system shows larger responsivity compared to individual wavelengths, the dynamic range of the system is rather small. Because of that, it turned out its fabrication tolerance is also small based on the simulation. We employed a three-laser system and redesigned the optical cavity to increase the dynamic range and improve the fabrication tolerance. In this presentation, we report the measurement results of the three-laser system for the first time. This system increases the dynamic range threefold by a chaining action. Because of this large dynamic range, this three-laser system is anticipated to have a larger fabrication tolerance.**

I. Introduction

Early diagnosis of diseases such as cancers significantly increases the chances of successful treatment [1-2]. Enzyme linked immunosorbent assay (ELISA) has been the gold standard for medical diagnosis. However, its high costs, complicated processes carried out by a skilled operator, and the need of large sample volumes limit this method to centralized clinical laboratories [3]. In this sense, point-of-care (POC) biosensors have emerged as a promising diagnostic tool for the early detection of diseases. A POC biosensor, which is used at or near the patients by patients' themselves, enables regular health monitoring without being dependent on the central laboratory testing. The successful development of a POC biosensor will greatly reduce fatalities and medical costs. To be an applicable platform for POC applications, the device is required to be cheap, label-free, accurate, and portable [4-5].

An optical cavity based biosensor using a differential calculation has been proposed for POC applications [7-9]. The light wave inside the optical cavity, formed by two partially reflective metal layers, travels back and forth due to the reflection from those mirrors so that the interference among multiple transmitted waves causes a resonance response. For the refractive index changes or the adsorption of biomolecules on surfaces inside the cavity, the resonance curve is shifted [6]. Unlike commonly used interferometric sensors which include a costly spectrometer or tunable laser to detect such changes or adsorption of biomolecules by measuring the resonance curve shift, we have proposed to use low cost laser diodes and detect their intensity changes due to the resonance curve shift using a CMOS camera. Also, to attain high sensitivity, we employed the differential calculation using two different wavelengths to increase responsivity and possibly reduce noise compared to individual laser diodes.

In order to experimentally validate our proposed system, the refractive index measurements have been performed using standard refractive index fluids (Cargille) from 1.3 to 1.395 with 0.005 interval. The light intensities, changing in accordance with the subjected refractive index fluids in the optical cavity, are measured and used to obtain the differential value. To fabricate an optical cavity structure, we started from two glass substrates. After coating a thin layer of silver on both substrates, an SU8 layer is patterned on top of the silver layer on both substrates and the two substrates are bonded together on the SU8 layer sides using a wafer-level SU8-to-SU8 bonding approach with heat and pressure to form an optical cavity structure [7]. Our device is designed to have a sensitivity near a refractive index of 1.33 in consideration of biosensing in the future. In the case of biological detection, target biomarkers in the sample fluid will attach to the functionalized surface, which in turn increases the refractive index near the surface from the index of the sample fluid close to 1.33 [10-11].

In this presentation, we will present the design and measurement results of two-laser system and simulation results showing the fabrication tolerance. Then, the design and measurement results of a three-laser system with a chaining action showing a large dynamic range will be presented.

II. Two-Laser System

A. Design and Simulation Results

The schematic diagram of a two-laser system is illustrated in Fig. 1. Two laser diodes at the wavelengths of 780nm and 850nm are used as light sources. Two collimated laser light waves are combined using a beam splitter and propagate through the optical cavity along the same path. The sCMOS camera measures the intensity one laser diode at a time.

We employed the differential detection method to enhance the responsivity. The equation to calculate differential values is given by (1), where η is a differential value, P_1 and P_2 are measured optical powers of the 780nm laser and 850nm laser, respectively.

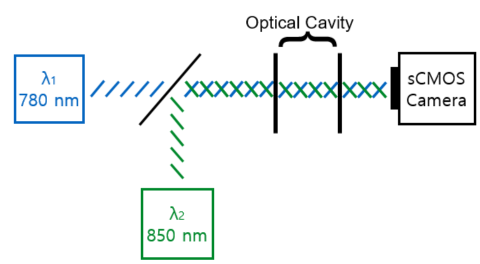

Figure 1. Schematic diagram of two-laser system [7].

*Research supported by National Science Foundation.

Donggee Rho and Seunghyun Kim are with the Electrical and Computer Engineering Department, Baylor University, Waco, TX 76798 USA. (phone: 254-710-4736; e-mail: Seunghyun_Kim@baylor.edu).

$$\eta = \frac{P_1 - P_2}{P_1 + P_2} \quad (1)$$

For two efficiencies changing monotonically in opposite directions, the differential value change is enhanced and larger than the changes in both wavelengths [7-9].

We used FIMMWAVE/FIMMPROP (Photon Design) software to design the optical cavity for the refractive index measurement. Fig. 2 shows the simulation results for a cavity width of 2.2 μm and a silver thickness of 11 nm, which shows the efficiencies of two wavelengths and the corresponding differential value with respect to the refractive index from 1.3 to 1.4. From 1.33 to 1.355, the differential value has a linear change with the slope of 44.496 /RIU (refractive index unit). Compared to this, the efficiencies of 780nm and 850nm show smaller slopes (23.789 /RIU and 25.07 /RIU, respectively) within smaller index ranges (1.35-1.368 and 1.322-1.34, respectively). The simulation results clearly show that the responsivity (change in values with respect to the refractive index change) and dynamic range (the refractive index range with a linear slope) of the differential values are better than an individual wavelength.

B. Measurement Results

Fig. 3 shows the refractive index measurement results showing the measured intensities of both wavelengths (780nm and 850nm) and calculated differential values from 1.3 to 1.345 refractive index. The intensity of 780nm is increasing in this range, while the intensity 850nm is decreasing as predicted in the simulation. Changing intensities in the opposite directions improved the responsivity of the differential value. Even though the measurement results look shifted slightly to the left, the results match very well with the simulation results. For instance, the differential value has 0.025 dynamic range (1.31 and 1.335) with a slope of 45.37/RIU, which is close to the simulation result 44.496 /RIU for the range of 1.33-1.355.

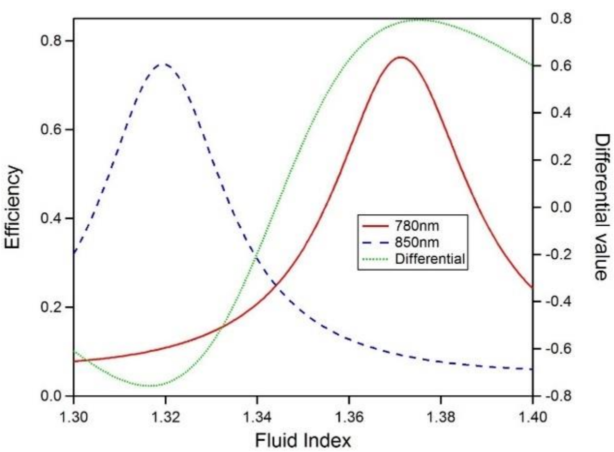

Figure 2. Simulation results of 2.2 μm cavity width with 11 nm silver thickness.

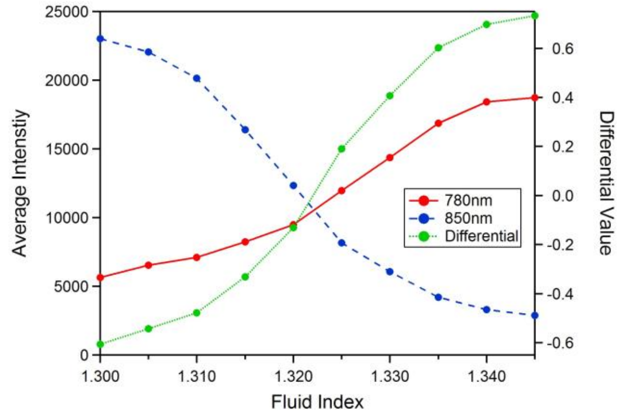

Figure 3. Measured intensities and differential values from 1.3 to 1.345.

C. Tolerance Analysis

We analyzed the fabrication tolerance for the cavity width to estimate its impact on the performance of our system through simulations. The results are shown in Fig. 4. A decrease or an increase in the cavity width by 50nm (2.15μm and 2.25μm respectively) from the desired width shifts the differential value response to either the right or left. The shift is large enough that the linear region does not include the refractive index of 1.33 anymore. Considering the biosensing scenario, this result means that the proposed optical cavity sensor doesn't have sensitivity if the cavity width is off by only 50 nm from the desired value. This tight tolerance is mainly due to the small dynamic range. If the dynamic range is large, even if the differential value response shifts from the desired one, it is possible to have a linear response near 1.33 always.

III. THREE-LASER SYSTEM

A. Design and Simulation Results

To increase the dynamic range and also improve the fabrication tolerance, we have proposed a three-laser system with a chaining action. Fig. 5 shows the schematic diagram of the three-laser system setup using laser diodes at wavelengths of 780nm, 808nm, and 904nm as light sources. The three collimated laser light waves are combined by two beam splitters into a single beam and propagate through the optical cavity along the same path. The sCMOS camera measures the intensity one laser diode at a time.

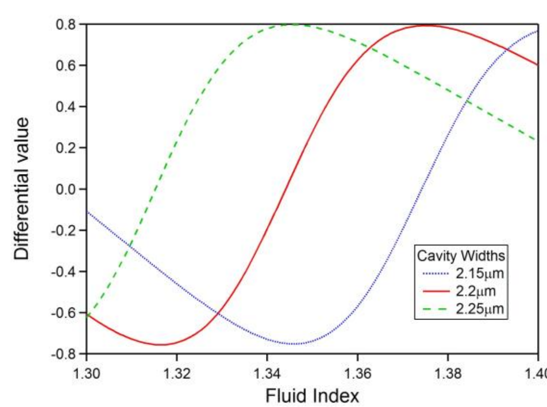

Figure 4. Differential values versus fluid index from 1.3 to 1.4 for 2.15μm, 2.2μm, and 2.25μm cavity widths.

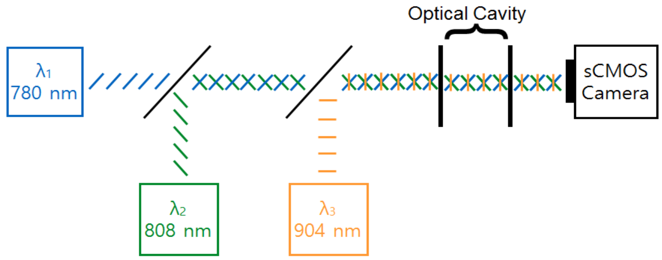

Figure 5. Schematic diagram of three-laser system.

The optical cavity is redesigned with these three wavelengths. The new optical cavity design has a cavity width of 3.5 μm and a silver thickness of 10 nm. Simulation results are shown in Fig. 6. The efficiency changes of the three wavelengths in between the refractive index range 1.3-1.5 overlap one another to form a repeating pattern. After selectively choosing the two wavelengths changing the most in the opposite directions, the differential values are calculated using them. For instance, 780nm and 808nm are selected to calculate the differential value between 1.308 and 1.33. Likewise, 780nm and 904nm are selected between 1.33-1.343 to calculate the differential value, and 808nm and 904nm are selected between 1.343-1.365. As shown in Fig. 7, the concatenated differential values at different refractive index ranges show the linear change over 1.308-1.44 (Δn=0.132). The combined differential values have a slope 25.275/RIU and a coefficient determination of 0.9987 (R^2). Compared to the two-laser system, the dynamic range is increased by more than 5 times.

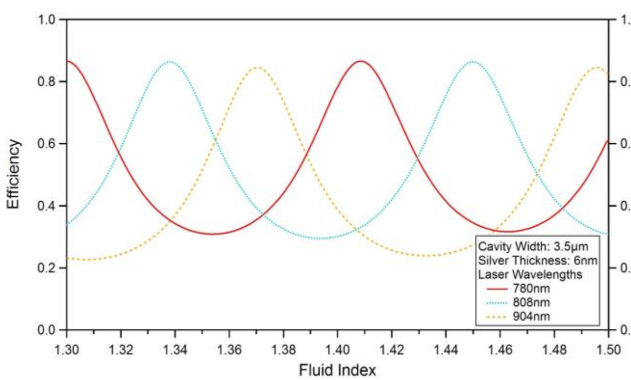

Figure 6. Three efficiencies versus refractive index from 1.3 to 1.5.

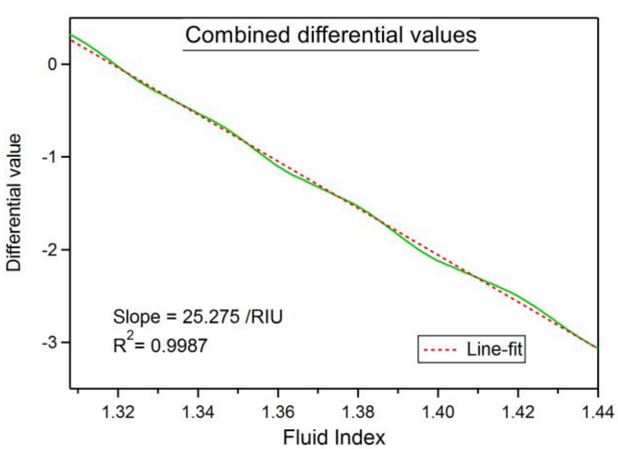

Figure 7. Combined differential values through chaining action.

B. Measurement Results

We used the same fabrication process except a shorter sputtering time for the silver layer and a slower spin speed for SU8 process to obtain the thicker layer. The optical test setup of the three-laser system is shown in Fig. 8.

Fig. 9 shows the measured intensities of 780nm, 808nm, and 904nm wavelengths in the refractive index range 1.31-1.395. As expected from the simulation, the intensities of three wavelengths show a continuous repeating pattern. For the chaining mechanism, two intensities are selected to calculate the differential value in a certain range. For the range of 1.31-1.325, 904nm and 780nm are used while 904nm and 808nm are used for the range 1.325-1.34. Intensities of 780nm and 808nm are used for 1.34-1.36 and 780nm and 904nm are used for 1.36-1.37. For the range of 1.37-1.39, 808nm and 904nm are used while 808nm and 780nm are used for the range of 1.39-1.395.

The concatenated differential values obtained with the chaining action in between the refractive index range of 1.31-1.395 are linearly changing, as shown in Fig. 10. The combined differential values have a slope of 29.741/RIU and a coefficient determination of 0.9951 (R^2). The measured dynamic range of the differential values is 0.085. We anticipate a larger fabrication tolerance with this large dynamic range because the differential value always changes linearly near 1.33, even if small errors in the cavity width may lead to a shift of the differential values.

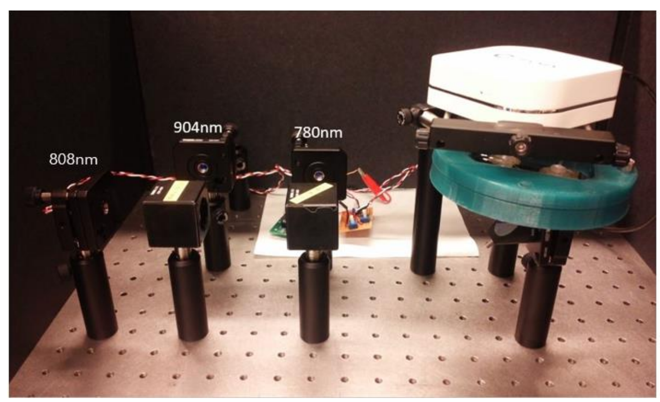

Figure 8. Test setup for three-laser system.

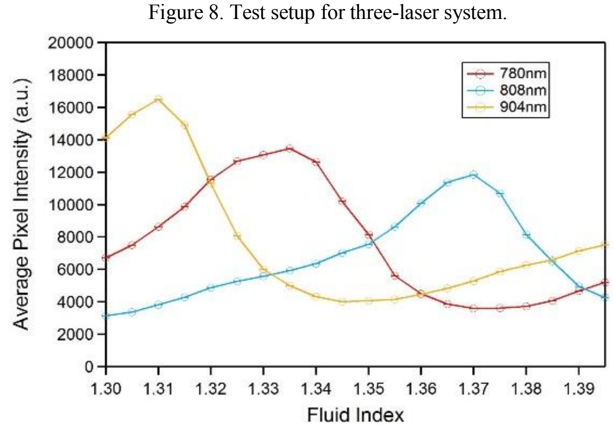

Figure 9. Measured intensities for 780nm, 808nm, and 904nm wavelengths.

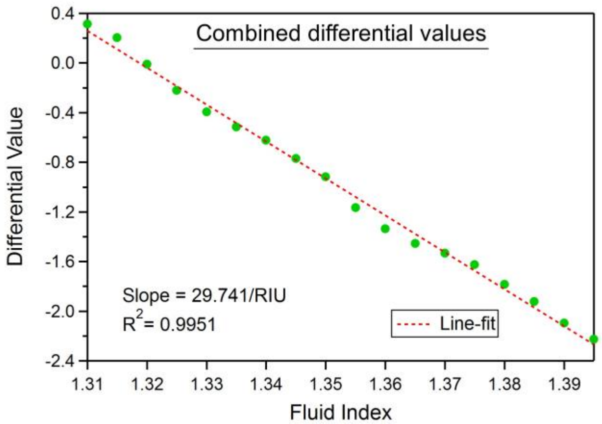

Figure 10. Combined differential value between 1.31 and 1.395.

IV. Conclusion

We have proposed and experimentally demonstrated an optical cavity based sensor with a differential detection method for the purpose of point-of-care applications. With the two-laser system, the experimental results show a higher responsivity (44.496 /RIU) and larger dynamic range ($\Delta n_{two\text{-}laser}$=0.025) compared to individual wavelengths. However, a tight fabrication tolerance is a weakness of the two-laser system. To improve it, we have designed the three-laser system. In this presentation, we report experimental measurement results of the three laser system for the first time. The concatenated differential values show the linear change in the refractive index range 1.31-1.395 ($\Delta n_{three\text{-}laser}$=0.085) which is more than 3 times larger than the two-laser system. Because of this large dynamic range, a large fabrication tolerance is also anticipated. In the future, by using the high affinity of biotin to streptavidin, biological tests will be performed to detect biotinylated BSA and determine its concentration.

Acknowledgment

This research has been supported by NSF grants CBET-1350648 and ECCS-1509799.

References

[1] R. Liu, Q. Wang, Q. Li, K. Yang, K. Wang, and W. Nie, "Surface plasmon resonance biosensor for sensitive detection of microRNA and cancer cell using multiple signal amplification strategy," *Biosensors and Bioelectronics*, vol. 87, pp. 433-438, Jan. 2017.

[2] Y. E. Choi, J. W. Kwak, and J. W. Park, "Nanotechnology for early cancer detection," *Sensors*, vol. 10(1), pp. 428-455, Jan. 2010.

[3] N. Garg, D. Vallejo, D. Boyle, I. Nanayakkara, A. Teng, J. Pablo, X. Liang, D. Camerini, A. P. Lee, and P. Felgner, "Integrated On-Chip Microfluidic Immunoassay for Rapid Biomarker Detection," *Procedia Engineering*, vol. 159, pp. 53-57, Aug. 2016.

[4] A. Gao, N. Lu, Y. Wang, and T. Li, "Robust ultrasensitive tunneling-FET biosensor for point-of-care diagnostics," *Scientific reports*, vol. 6, Mar. 2016.

[5] A. S. Vasan, D. M. Mahadeo, R. Doraiswami, Y. Huang, and M. Pecht, "Point-of-care biosensor system," *Frontiers in bioscience (Scholar edition)*, vol. 5, pp. 39-71, Jan. 2013.

[6] A. A. P. Trichet, J. Foster, N. E. Omori, D. James, P. R. Dolan, G. M. Hughes, C. Vallance, and J. M. Smith, "Open-access optical microcavities for lab-on-a-chip refractive index sensing," *Lab on a Chip*, vol. 14(21), pp. 4244-4249, Sep. 2014.

[7] D. Rho, S. Cho, C. Joy, and S. Kim, "Demonstration of an optical cavity sensor with a differential detection method by refractive index measurements," in *Proc. Wireless and Microwave Circuits and Systems (Texas Symposium*), Texas, 2015, pp. 1–4.

[8] S. Cho, J. H. Brake, C. Joy, and S. Kim, "Refractive index measurement using an optical cavity based biosensor with a differential detection," in *Proc. SPIE BiOS,* 2015, p. 93320Z.

[9] P. Cowles, C. Joy, A. Bujana, D. Rho, and S. Kim, "Preliminary measurement results of biotinylated BSA detection of a low cost optical cavity based biosensor using differential detection," in *Proc. SPIE BiOS,* 2016, p. 972509.

[10] C. Novo, A. M. Funston, I. Pastoriza-Santos, L. M. Liz-Marzan, and P. Mulvaney, "Influence of the medium refractive index on the optical properties of single gold triangular prisms on a substrate," *The Journal of Physical Chemistry C*, vol. 112(1), pp. 3-7, 2008.

[11] S. Zhu, F. Pang, S. Huang, F. Zou, Y. Dong, and T. Wang, "High sensitivity refractive index sensor based on adiabatic tapered optical fiber deposited with nanofilm by ALD," *Opt. Express*, vol. 23(11), pp. 13880-13888, May 2015.